

The Vernadsky scale – on metrology of EIS in time-frequency domain

S.Kernbach, I.Kuksin, O.Kernbach, A.Kernbach

Abstract—The paper briefly considers the metrology of electrochemical impedance spectroscopy (EIS) in the time-frequency domain, in particular the choice of scales and units of measurements. The usage of dimensionless, $func(t)^{-1}$ or $func(f, t)^{-1}$ scales is analysed in relation to stationarity of measurement process. A method of reproducible calibration of EIS devices for standardization of such measurements is described. Examples of influencing a liquid cell by physical and biological objects as well as by the environment are shown. It is proposed to support the initiative of naming the measurement scale of weak emissions as the Vernadsky scale.

I. INTRODUCTION

Electrochemical impedance spectroscopy (EIS) is a well-known method of physicochemical analysis in laboratory, field and industrial environments [1], [2]. The first applications of this method for measurements of weak emissions refer to the 80s [3]. At present, the EIS is developed further, in particular, the impedance spectroscopy is applied not only in the frequency domain, but also in the time-frequency domain. Such EIS measurements



Fig. 1. The differential EIS spectrometer, 1,2,3 – elements of the device; 4, 5 – electrodes of the channel 1 and 2.

Cybertronica Research, Research Center of Advanced Robotics and Environmental Science, Melunerstr. 40, 70569 Stuttgart, Germany, Contact author: serge.kernbach@cybertronica.de.com, translation from original paper.

are carried out with a long-term exposition of the fluidic system by electrical excitation signals without removing electrodes from measuring containers, see Fig. 1. In this method, the sensory element is represented not only by the physicochemical properties of fluids, but also by electrochemical interactions during measurements, which utilize several quantum mechanisms on the level of ion production and proton conductivity [4], [5], [6]. This methodology significantly increases the sensitivity and resolution of the sensor, as well as minimizes interferences.

Measurements in the time-frequency domain extend the EIS paradigm for investigating a stationarity of fluids. In this case, it is common to consider the measuring system as a linear stationary system for small signals with discrete time [7]. The analysis is performed by the frequency response analysis (FRA), as well as by processing the RMS excitation and response signals [8]. Both methods are implemented in the EIS device and in the measurement methodology.

The time-frequency EIS introduces in fact a new scale and it is necessary to consider metrological issues of these measurements. First of all, the question arises about the used measurement scales and calibration of EIS devices. The following sections consider the application of dimensionless, $func(t)^{-1}$ or $func(f, t)^{-1}$ scales. We argue that all three options reflect the same principle of relative measurements, described in [9]. Since Prof. Vernadsky was one of the first researchers, who expressed in 1931 [10] the idea of a common unit in measuring various weak emissions, it is proposed to support the initiative of naming this scale as the Vernadsky scale.

II. SPECTROSCOPY IN THE TIME-FREQUENCY DOMAIN

The result of EIS analysis in the time-frequency domain is represented by the third-rank tensor ${}^k\Upsilon_t^f$ with discrete indices k, f, t . The f, t denote the frequency and time components, the index k denotes the components of EIS analysis (magnitude, phase, correlation, real and imaginary parts of the FRA, etc.), see [11] on the tensor notation. The dimension ${}^k\Upsilon_t^f$ causes difficulties for its representation, one of the possibilities is to use the heat map graphs, where t, f are located on the axes x, y , and the color scale represents one of k , see Fig. 2. The tensor ${}^k\Upsilon_t^f$ has the following form

CYBRES EIS, Device ID:322016, Heat map of RMS conductivity, ch.1 (Normal Scale)

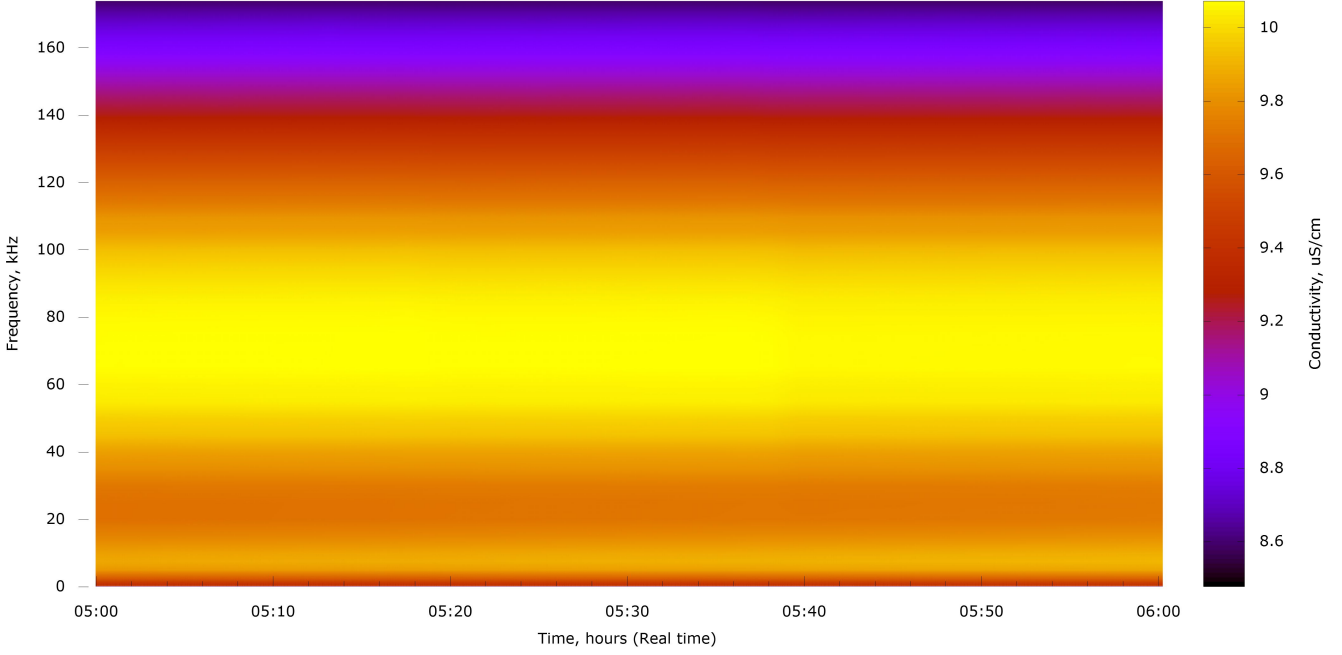


Fig. 2. Graphical representation of the tensor ${}^k\Upsilon_t^f$ (1) as the heat map, color palette RGB, the conductivity of water is measured in the frequency range 0.1kHz–170kHz.

$$\begin{array}{cccc|cccc}
 {}^k\Upsilon_{t_0}^{f_{max}} & {}^k\Upsilon_{t_1}^{f_{max}} & \dots & {}^k\Upsilon_{t_{m-1}}^{f_{max}} & {}^k\Upsilon_{t_m}^{f_{max}} & {}^k\Upsilon_{t_{m+1}}^{f_{max}} & \dots & {}^k\Upsilon_{t_{max-1}}^{f_{max}} & {}^k\Upsilon_{t_{max}}^{f_{max}} \\
 {}^k\Upsilon_{t_0}^{f_{max-1}} & {}^k\Upsilon_{t_1}^{f_{max-1}} & \dots & {}^k\Upsilon_{t_{m-1}}^{f_{max-1}} & {}^k\Upsilon_{t_m}^{f_{max-1}} & {}^k\Upsilon_{t_{m+1}}^{f_{max-1}} & \dots & {}^k\Upsilon_{t_{max-1}}^{f_{max-1}} & {}^k\Upsilon_{t_{max}}^{f_{max-1}} \\
 \dots & \dots \\
 {}^k\Upsilon_{t_0}^{f_2} & {}^k\Upsilon_{t_1}^{f_2} & \dots & {}^k\Upsilon_{t_{m-1}}^{f_2} & {}^k\Upsilon_{t_m}^{f_2} & {}^k\Upsilon_{t_{m+1}}^{f_2} & \dots & {}^k\Upsilon_{t_{max-1}}^{f_2} & {}^k\Upsilon_{t_{max}}^{f_2} \\
 {}^k\Upsilon_{t_0}^{f_1} & {}^k\Upsilon_{t_1}^{f_1} & \dots & {}^k\Upsilon_{t_{m-1}}^{f_1} & {}^k\Upsilon_{t_m}^{f_1} & {}^k\Upsilon_{t_{m+1}}^{f_1} & \dots & {}^k\Upsilon_{t_{max-1}}^{f_1} & {}^k\Upsilon_{t_{max}}^{f_1} \\
 {}^k\Upsilon_{t_0}^{f_0} & {}^k\Upsilon_{t_1}^{f_0} & \dots & {}^k\Upsilon_{t_{m-1}}^{f_0} & {}^k\Upsilon_{t_m}^{f_0} & {}^k\Upsilon_{t_{m+1}}^{f_0} & \dots & {}^k\Upsilon_{t_{max-1}}^{f_0} & {}^k\Upsilon_{t_{max}}^{f_0}
 \end{array} \quad (1)$$

The tensor ${}^k\Upsilon_t^f$ is structured with respect to the indices t for the areas before and after the time t_m

$$A : {}^k\Upsilon_t^f \rightarrow t < t_m, \quad (2)$$

$$B : {}^k\Upsilon_t^f \rightarrow t \geq t_m, \quad (3)$$

where t_m represents the begin of exposure, A is the background measurement area, and B is the area, where the response is analyzed.

An essential issue of ${}^k\Upsilon_t^f$ in relation to components f is the superposition of the response of EIS system U_{EIS} and the response of a fluidic test object U_{object}

$${}^k\Upsilon^{f=f_0\dots f_{max}} = U_{EIS}^f U_{object}^f. \quad (4)$$

In some EIS systems [12] a linear character U_{EIS}^f of f is assumed and an offset calibration for $f = f_0\dots f_{max}$ is performed. This leads U_{EIS}^f to 1 for all f . However, the real properties of U_{EIS}^f are non-linear, thus the expression (4) results in a non-linear sensitivity, manifested in different scales for each of f . This effect is well visible in Fig. 2,

where the difference between f is much larger than the variation of the signal inside one f .

The behavior of ${}^k\Upsilon_t^f$ in relation to the components t results in nonlinearity, due to the fact that EIS interacts with the test system during measurements

$${}^k\Upsilon_{t=t_0\dots t_{max}} = O_t^{EIS} \left(O_t^{object}, t \right). \quad (5)$$

An example of such an interaction is the self-ionization, where the external electric field changes equilibrium condition of dissociation and recombination of H_3O^+ and H^- [13]. As mentioned above, the mechanism of self-ionization is of quantum nature [5] (among other factors). It should be noted that the expression (5) can include different components, such as a non-stationarity of fluidic cell and weak emission, as well as a non-stationarity of the measurement itself. These components should be distinguished from each other.

Let us consider one of the components k , represented, for example, by the magnitude of impedance $Z(f, t)$ with the dimension $Om \cdot m$. The measurement of this value by the

CYBRES EIS, Device ID:322016, Heat map of RMS conductivity, ch.1 (Vernadsky Scale of Relative Measurements)

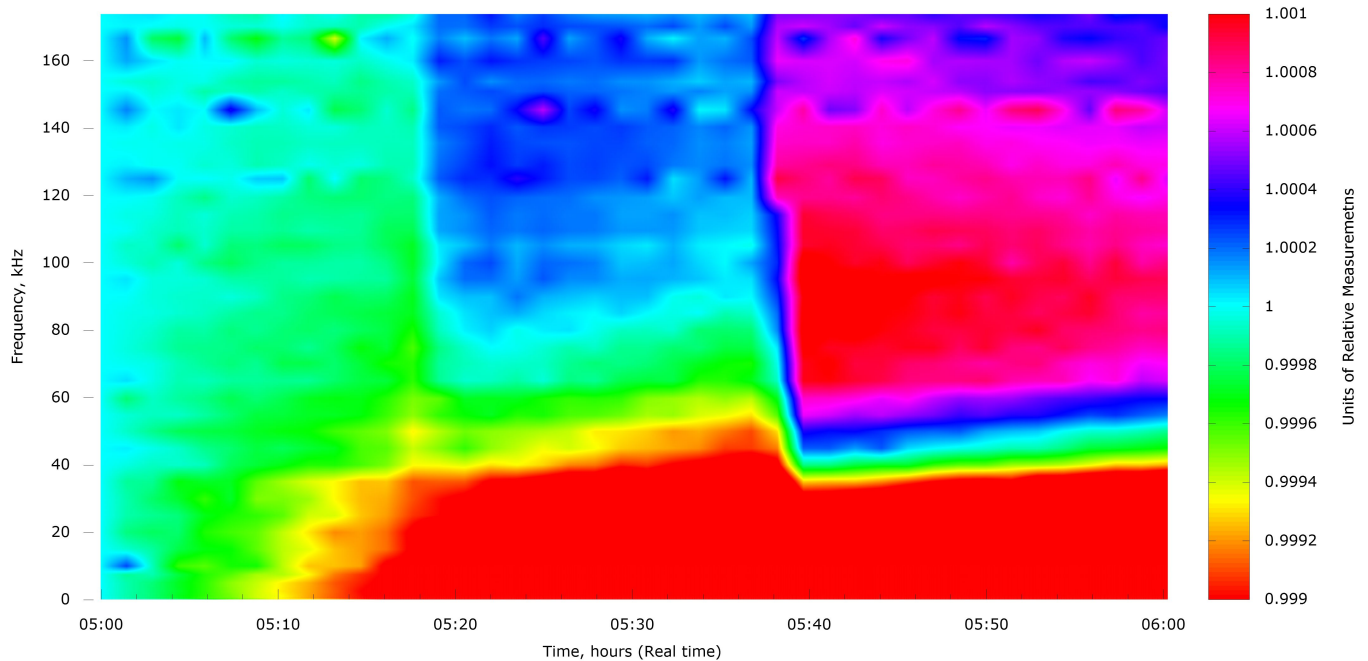


Fig. 3. The normalized representation of the tensor ${}^k\Upsilon_t^f$ by (8). The same graph as in Fig. 2, but represented in the Vernadsky scale, the color palette HSV, the resolution $2 \cdot 10^{-3}$ URM for the entire scale, conductivity fluctuations at 10^{-4} URM (Units of Relative Measurements) are well visible, the temperature of fluidic cell is stabilized.

RMS approach consists in analyzing the excitation signal $V_V(f, t)$ and the current response signal $V_I(f, t)$

$$Z(f, t) = s(f) \frac{V_V(f, t)}{V_I(f, t)}, \quad (6)$$

where $s(f)$ is the cell constant, defined as the ratio between the area of electrodes to the distance between them (considering the geometry of the cell). Since the impedance of a two-terminal network should be independent of time, the following agreement is used – the measurement (6) should be performed in a short time, so that the non-linear part of (5) remains small and can be neglected for the given measurement accuracy

$$Z(f, t) = s(f) \frac{V_V(f, t)}{V_I(f, t)} \xrightarrow{t \rightarrow 0} Z(f) = s(f) \frac{V_V(f)}{V_I(f)}. \quad (7)$$

To avoid the nonlinearity in $s(f)$, the frequency f is often fixed. For example, the cell constant is calibrated in this way. It is obvious that (7) and (1) to some extent represent different EIS paradigms, because (1) affects the stationarity of physical quantities indexed by k .

III. NORMALIZATION OF THE RESPONSE OF THE TEST SYSTEM

Spectroscopy in the form (1) is not used in cases where the structures (2) and (3) are not distinguished from each other, and the method (7) is more preferable. However, in applications where the structures (2) and (3) should be distinguished, it is necessary to solve the above-mentioned problems of ${}^k\Upsilon_t^f$ in the form of different scales in the index

f and a violation of stationarity in the index t . The work [9] already expressed the idea that the structure (2) in ${}^k\Upsilon_t^f$ represents an independent physical quantity characterizing the reaction of test system without an external stimulus. In order to avoid different scales in f , it was suggested to make ${}^k\Upsilon_t^f$ in the area A (2) dimensionless with respect to physical quantities in k , for example, in the form

$$\varphi^A = \frac{{}^k\Upsilon_t^{f=f_0 \dots f_{max}}}{{}^k\Upsilon_{t_0}^{f=f_0 \dots f_{max}}} = f_{unc}(f, t), \quad t < t_m, \quad (8)$$

so that

$$\varphi^A(f, t) \approx 1, \quad t < t_m. \quad (9)$$

This representation is shown in Fig. 3. The value of t_m is chosen to satisfy (9), which is implemented as a sliding window. Fig. 6 shows the application of (9) to the region B (the dynamics after impact), where the sliding window method allows showing time-frequency patterns at the deviation level 10^{-3} URM for all f . In this case, the approximation accuracy (to the 1) of the unexcited state of the EIS system can be defined, for example, the deviation values $10^{-4} - 10^{-5}$ URM are achievable. Considering (9) from the metrological point of view, we can note that (8) acts as a normalizing metric operator with (9) as a unit scale. Although $\varphi(f, t)$ is a function of frequency and time, the normalization (9) makes it, and correspondingly the entire scale, dimensionless that satisfies the assumptions made in [9].

Now we consider the structure (3) in ${}^k\Upsilon_t^f$. Its physical meaning is the reaction of test system in the context of physical quantities indexed by k . Here the normalization

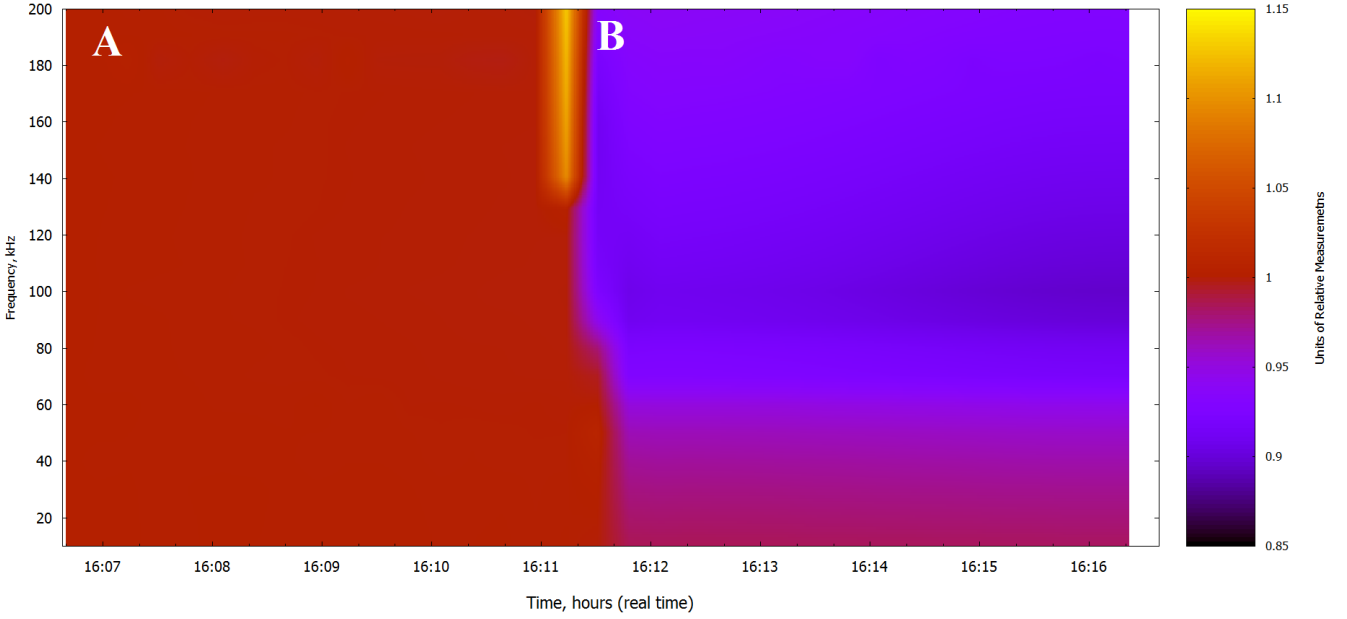


Fig. 4. The normalized representation of the tensor $k\varphi_t^f$ by (14) with structures (2) (the region A before exposure) and (3) (the region B after begin of exposure). The exposure performed by a biological object (touching by a hand for 5 seconds).

(9) can not be performed. There are two ways of considering the structure (3) with respect to the structure (2) (the unit scale). In the first case, we extend (8) to all values of t

$$\varphi^B = \frac{k\Upsilon_t^{f=f_0\dots f_{max}}}{k\Upsilon_{t_0}^{f=f_0\dots f_{max}}} \Big|_{t=t_w} = func(f), \quad t \leq t_{max}, \quad (10)$$

by fixing the time $t = t_w$ in the manner (7). In this method, the entire response of the test system represents the sum of responses at short discrete instants of time, i.e. the value t is replaced by a measurement index. An example can be given by the Nyquist diagram, which does not include time but can be indexed by the number of its measurement. This approach solves the problem of measurement stationarity since all indexed values are in fact independent measurements performed in the manner of expression (7).

In the second case, we consider (8) only for $t \geq t_m$

$$\varphi^B = \frac{k\Upsilon_t^{f=f_0\dots f_{max}}}{k\Upsilon_{t_0}^{f=f_0\dots f_{max}}} = func(f, t), \quad t \geq t_m. \quad (11)$$

Here the whole system is considered as non-stationary in sense of (5) and the dynamics of physical quantities in the index k is investigated. For example, the conductivity dynamics measured by the RMS method can be considered.

Despite the similarity, the (10) and (11) have different metrological and physical meaning, since they lead to different dimensions of the total φ for $t \leq t_{max}$

$$\varphi = \varphi^B, \quad t \leq t_{max}, \quad (12)$$

and

$$\varphi = \frac{\varphi^A}{\varphi^B} = \frac{1}{\varphi^B}, \quad t \leq t_{max}, \quad (13)$$

Both variants convert (10) to the form

$$\begin{array}{cccc|cccc} 1 & 1 & \dots & 1 & k\varphi_{t_m}^{f_{max}} & k\varphi_{t_{m+1}}^{f_{max}} & \dots & k\varphi_{t_{max-1}}^{f_{max}} & k\varphi_{t_{max}}^{f_{max}} \\ 1 & 1 & \dots & 1 & k\varphi_{t_m}^{f_{max-1}} & k\varphi_{t_{m+1}}^{f_{max-1}} & \dots & k\varphi_{t_{max-1}}^{f_{max-1}} & k\varphi_{t_{max}}^{f_{max-1}} \\ \dots & \dots \\ 1 & 1 & \dots & 1 & k\varphi_{t_m}^{f_2} & k\varphi_{t_{m+1}}^{f_2} & \dots & k\varphi_{t_{max-1}}^{f_2} & k\varphi_{t_{max}}^{f_2} \\ 1 & 1 & \dots & 1 & k\varphi_{t_m}^{f_1} & k\varphi_{t_{m+1}}^{f_1} & \dots & k\varphi_{t_{max-1}}^{f_1} & k\varphi_{t_{max}}^{f_1} \\ 1 & 1 & \dots & 1 & k\varphi_{t_m}^{f_0} & k\varphi_{t_{m+1}}^{f_0} & \dots & k\varphi_{t_{max-1}}^{f_0} & k\varphi_{t_{max}}^{f_0} \end{array} \quad (14)$$

Although φ in (12) is a function of frequency, in fact both time and frequency are represented by discrete measurement indexes. In the physical sense the expression (10) leads φ to an indexed dimensionless value. On the

other hand, φ in (13) has a dimension $func(f, t)^{-1}$ that with similar consideration of frequency as the indexed parameter can lead to $func(t)^{-1}$. Both options are already mentioned in the literature, e.g. [9], [14] expressed argu-

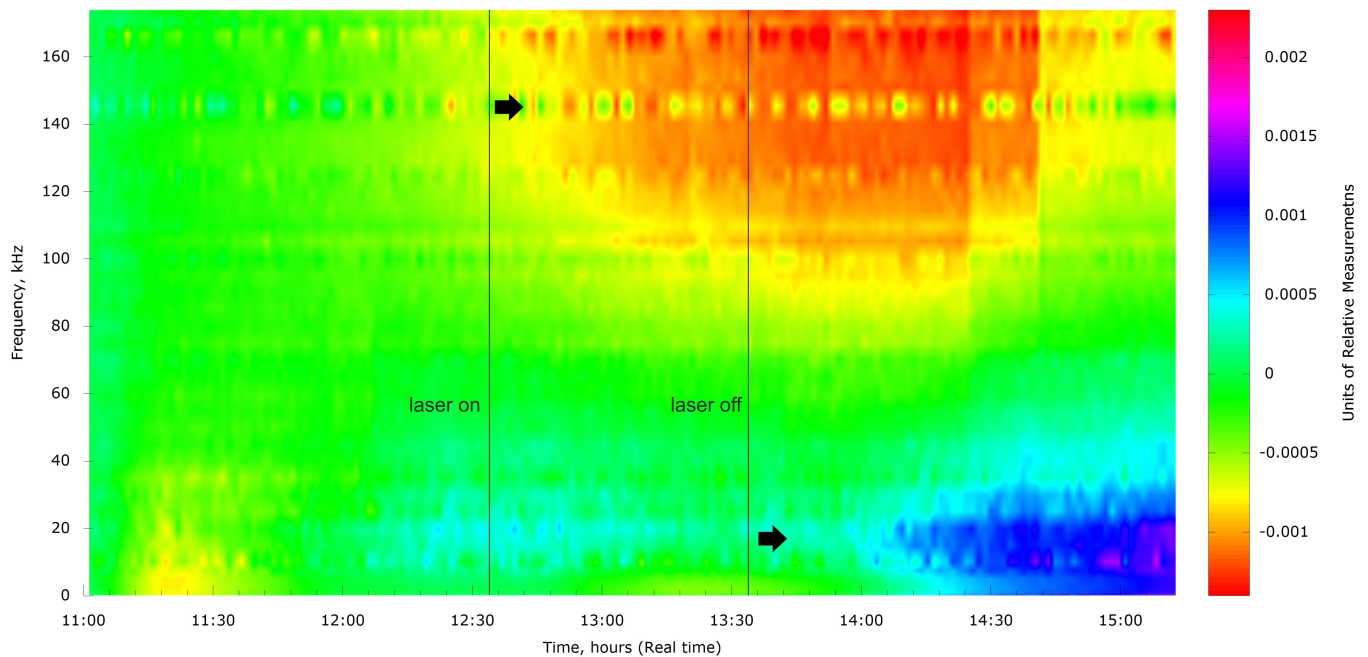


Fig. 5. The impact of a laser (512nm, 5mV, the class 1) on a liquid in the channel 1 through a sugar cube (the liquid is completely closed from exposure to laser light), the channel 2 is placed behind the channel 1 at the distance of 10 cm. The differential dynamics of channels before, during and after the exposure is shown, the color palette HSV, the resolution $3 \cdot 10^{-3}$ URM for the whole scale. The appearance of high-frequency components after switching on the laser and low-frequency components after switching off is visible. The renormalization ${}^k\varphi_t^f$ is performed at the beginning of measurement.

ments in favor of the dimensionless φ , while [15], [16], [17] considered the option sec^{-1} for φ .

IV. DIMENSION φ : DIMENSIONLESS QUANTITY, $func(t)^{-1}$ OR $func(f,t)^{-1}$?

The physical meaning of φ for $t \leq t_{max}$ consists either in characterization of the test object (when the impact is known), or in characterization of the impact (when test object is known). Both variants are used in practical tasks. In our case, with a known test object (distilled water of a certain standard with given measurement parameters), it is possible to characterize the source of weak emission. It seems more logical to use the dimensionless variant of calculating φ , as *the ratio of the behavior of non-impacted test system to the behavior of impacted test system*. It is necessary to fix the time of impact $t = t_w$. In fact, the entire scale based on normalization (8) and (9), and proposed in [9] is dimensionless. The situation with dimensionless scales has not changed in the last 20 years of research [14].

Dimensionless scales have strengths and weaknesses. For example, without theoretical foundation of weak emissions that is accepted by most researchers, and with increasing role of quantum effects in macro-systems, a dimensionless scale remains only one realistic possibility for calibrating measurement devices. Dimensionless scales allow measuring the steady-state characteristics in the response of test systems. However, when considering the dynamics of these

responses for $t \geq t_m$, for example, the attenuation values, it is necessary to take $func(f,t)^{-1}$ for φ .

The obvious difficulty of introducing $func(f,t)^{-1}$ is an unclear physical meaning of this dimension. The [15], [16] provided arguments for $func(t)^{-1}$ with the rotation of objects or the torsion fields, which are too complex for solving metrological problems in real devices. Taking into account the quantum phenomena that participate in the measurement of weak emissions, the physical meaning of the dimension $func(t)^{-1}$ as well as $func(f,t)^{-1}$ is even more unclear.

An essential argument for the choice of scales is a stationarity of measurement processes (to distinguish with the stationarity of the test system and the impact). Criticism of [15] and similar works is the loss of measurement stationarity, i.e. repeated measurements of one object under the same conditions may not lead to the same result. This is not acceptable for practical measurements. The method (7) guarantees stationarity for measurements, which leads to the selection of (10) and (12) in calculation of φ for $t \leq t_{max}$. This results in a dimensionless scale represented on the corresponding axis as 'Units of Relative Measurements' (URM).

In conclusion of this section, we would like to quote the words of V.I.Vernadsky: 'On the basis of new physics, the phenomenon should be studied in a space-time domain. The space of life, as we have seen, has its own special state in nature. The time that corresponds to it has not only the polar character, but also a special parameter

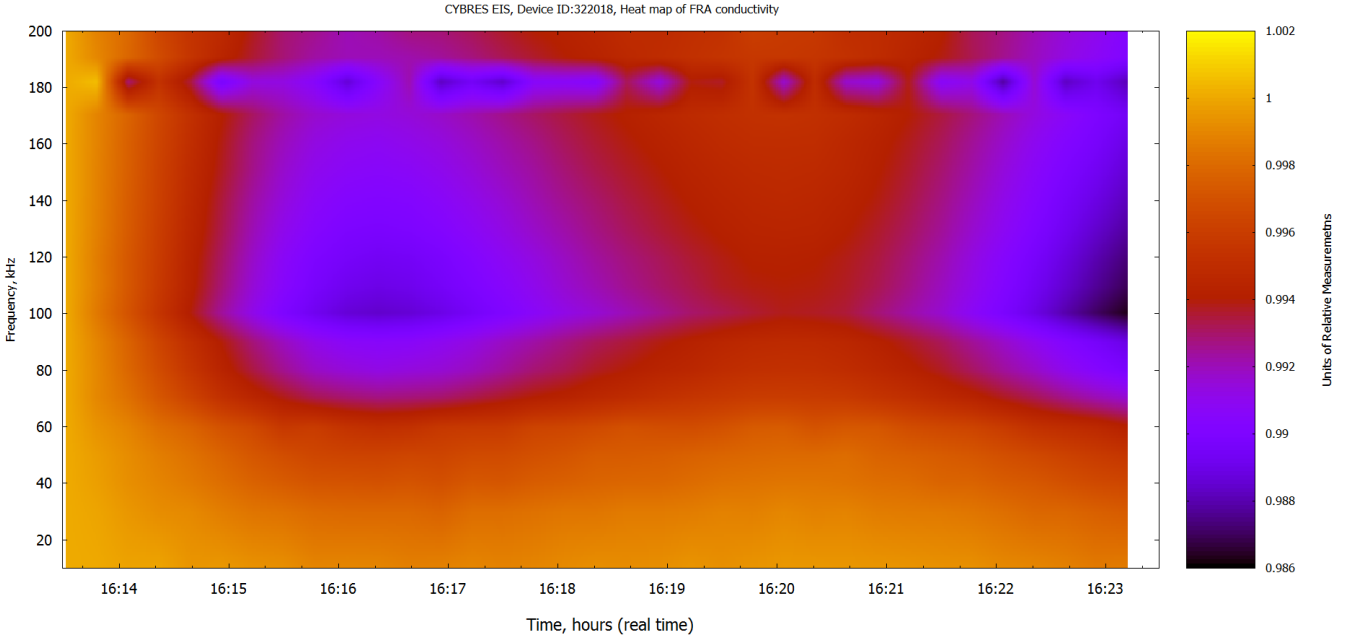


Fig. 6. Appearance of post-experimental time-frequency structures in a test fluid upon renormalization of ${}^k\varphi_t^f$ in a sliding analysis window, the color palette RGB.

peculiar to it, a unit of measurement, which is related to life' [10]. To demonstrate the special meaning of the scale associated with measurements of weak emissions, and by following [14], [15], it is suggested to name this scale as the Vernadsky scale.

V. THE MEANING OF THE VERNADSKY SCALE

The proposal for naming the scale of relative measurements as the Vernadsky scale refers to the 90s of the 20th century and is related to activities of A.E.Akimov, P.I.Goskov and other researchers. Reflections on the role of Vernadsky in the *noosphere research* and weak emissions can also be found in the works of V.P.Kaznacheev and A.V.Trofimov [18]. From a philosophical point of view, these works reflect the trends of *cosmism* – the holistic worldview of an ordered universum and of a man as a microcosm. In these works, a person is considered as a unit of the noospheric evolution, which proceeds both in the physical world and in a special (perhaps informational) dimension, called by Kaznacheev as the 'Kozyrev's dimension'. Various social, economic and technological processes are normalized (or quantized) by unit of this process - the 'monad of a man' (in the noosphere terminology). To some extent this reflects the principle of the relativity – everything that happens is interpreted within the framework of a single 'noospheric carrier'. For all the heterogeneity and diversity of such 'individual carriers', the whole process in its totality will give more or less similar results, allowing them to be compared with each other. Ideas of *cosmism* are much deeper, but in application to measurements of weak emissions they reflect three essential points:

1. Recognition of the fact of differences (or even uniqueness) of 'individual carriers' and their manifestations in physical and information dimension.
2. Normalization of measured processes on a single 'carrier'.
3. Considering the whole picture of the normalized 'carriers'.

It is obvious that the Vernadsky scale differs from absolute measurement scales. The problem of measurements is the 'individual carrier' – how to find it and to measure it. We propose to consider each measurement process as a 'single carrier', where the normalization is performed on the behavior of the test system prior to the impact.

We can give an example. Let the changes in conductivity (phase, correlation, pH, etc.) in the phase *B* (after the impact) be at 0.999–1.001 in the Vernadsky scale. These values are obtained according to (10) and (12) as the ratio of conductivity in the experimental region to the conductivity in the background region. In absolute scale, if the conductivity of used water is 2 $\mu\text{S}/\text{cm}$, this means that the variation in experimental region will be $2 \cdot (1.001 - 0.999) = 0.004 \mu\text{S}/\text{cm}$ or 4nS/cm. Values in the Vernadsky scale allow avoiding different physical quantities and focusing on their relative changes under weak emissions. It should be remembered that these quantities are meaningful only when considering the whole picture, i.e. with accumulation of statistics from different impacts and different test systems.

VI. CALIBRATION OF EIS

The expression (9) defines the meaning of calibration, its value for $t \leq t_m$ should approach 1 with the deviation $10^{-3} - 10^{-5}$. It is proposed to use technical demineralized

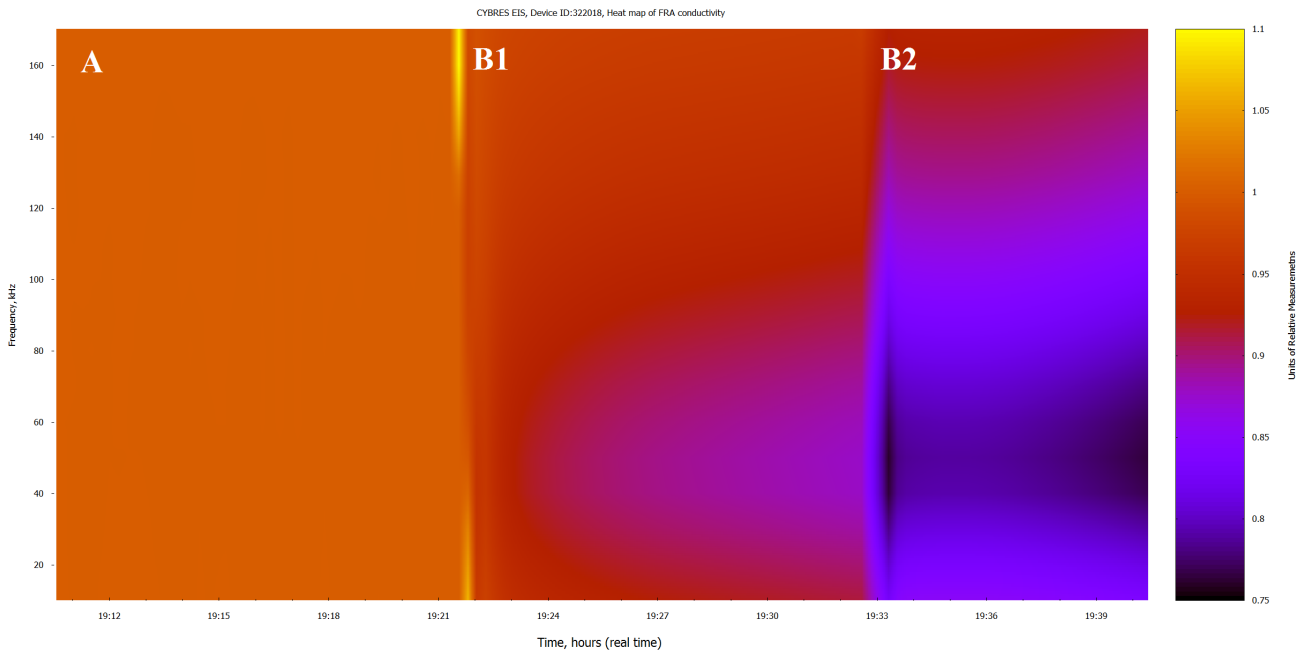


Fig. 7. Two impacts (B1, B2) by biological objects on the test fluid without repeated renormalization ${}^k\varphi_t^f$, the differences in the time-frequency properties of both impacts are clearly visible.

water (for example, meeting the standards of DIN 43530-4, VDE 0510 or similar) at room temperature 22-32°C as a test object. It is necessary to measure the temperature of liquids (small changes in conductivity can be compensated by means of temperature coefficients). The conductivity of water must be $> 1\mu S/cm$ and $< 3\mu S/cm$ (therefore it is necessary to control storage conditions with respect to CO_2). It is necessary to exclude light and EM fields from measurements. An essential issue for calibration is the stationarity condition of the measuring liquid. Omitting the discussion about whether the EIS is stationary in a long time, we point to (7) as a condition for achieving stationarity at such time intervals when (9) is satisfied. In other words, measurements should be conducted with fresh water taken from a large container, the longer the measurement lasts, the greater is the non-stationarity the test fluid. It should be remembered that the exposure of a liquid by experimental factors (weak emissions or other phenomena) is also not stationary in many cases, therefore, EIS measurements have a probabilistic character. It is necessary to carry out a minimum number of independent measurements (30 attempts) under similar conditions to obtain a statistically significant result.

From a practical point of view, the renormalization of ${}^k\varphi_t^f$ can be carried out in a sliding window, and the resolution of post-experimental dynamics is significantly increased, as for example shown in Fig. 6. On the other hand, without renormalization, it is possible to compare the parameters of two different effects, as shown in Fig. 7, 5 or as 4D graph in Fig. 8.

REFERENCES

- [1] S. Kernbach, I. Kuksin, and O. Kernbach. Analysis of ultraweak interactions by electrochemical impedance spectroscopy (rus). *IJUS*, 11(4):6–22, 2016.
- [2] S. Kornienko, O. Kornienko, and P. Levi. Multi-agent repairer of damaged process plans in manufacturing environment. In *Proc. of the 8th Conf. on Intelligent Autonomous Systems (IAS-8), Amsterdam, NL*, pages 485–494, 2004.
- [3] V.A. Sokolova. *First experimental confirmation of torsion fields and their usage in agriculture (rus)*. Moscow, 2002.
- [4] Jeremy O. Richardson, Cristóbal Pérez, Simon Lobsiger, Adam A. Reid, Berhane Temelso, George C. Shields, Zbigniew Kisiel, David J. Wales, Brooks H. Pate, and Stuart C. Althorpe. Concerted Hydrogen-Bond Breaking by Quantum Tunneling in the Water Hexamer Prism. *Science*, 351(6279):1310–1313, March 2016.
- [5] P. L. Geissler, C. Dellago, D. Chandler, J. Hutter, and M. Parrinello. Autoionization in Liquid Water. *Science*, 291:2121–2124, March 2001.
- [6] J.O.M. Bockris and A.K.N. Reddy. *Modern Electrochemistry: An Introduction to an Interdisciplinary Area*. Number Bd. 2 in A Plenum/Rosetta edition. Springer US, 1973.
- [7] J.P. Hespanha. *Linear System Theory*. Princeton university press, 2009.
- [8] S.Kernbach and O.Kernbach. Reliable detection of weak emissions by the EIS approach. *IJUS*, 14(4):65–79, 2017.
- [9] S. Kernbach. On metrology of systems operating with 'high-penetrating' emission (rus). *International Journal of Unconventional Science*, 1(2):76–91, 2013.
- [10] V.I. Vernadsky. *Studying the phenomena of life and the new physics (1931) (Rus)// Proceedings on biogeochemistry and geochemistry of soils*. Moscow, 1992.
- [11] P. Levi, M. Schanz, S. Kornienko, and O. Kornienko. Application of order parameter equation for the analysis and the control of nonlinear time discrete dynamical systems. *Int. J. Bifurcation and Chaos*, 9(8):1619–1634, 1999.
- [12] S. Kernbach, I. Kuksin, and O. Kernbach. On accurate differential measurements with electrochemical impedance spectroscopy. *WATER*, 8:136–155, 2017.
- [13] J.Koryta and J.Dvorak. *Principles of Electrochemistry*. John Wiley & Sons Ltd, 1987.

CYBRES EIS, Device ID:322018, Heat map of FRA phase, ch.1 (Vernadsky Scale of Relative Measurements)

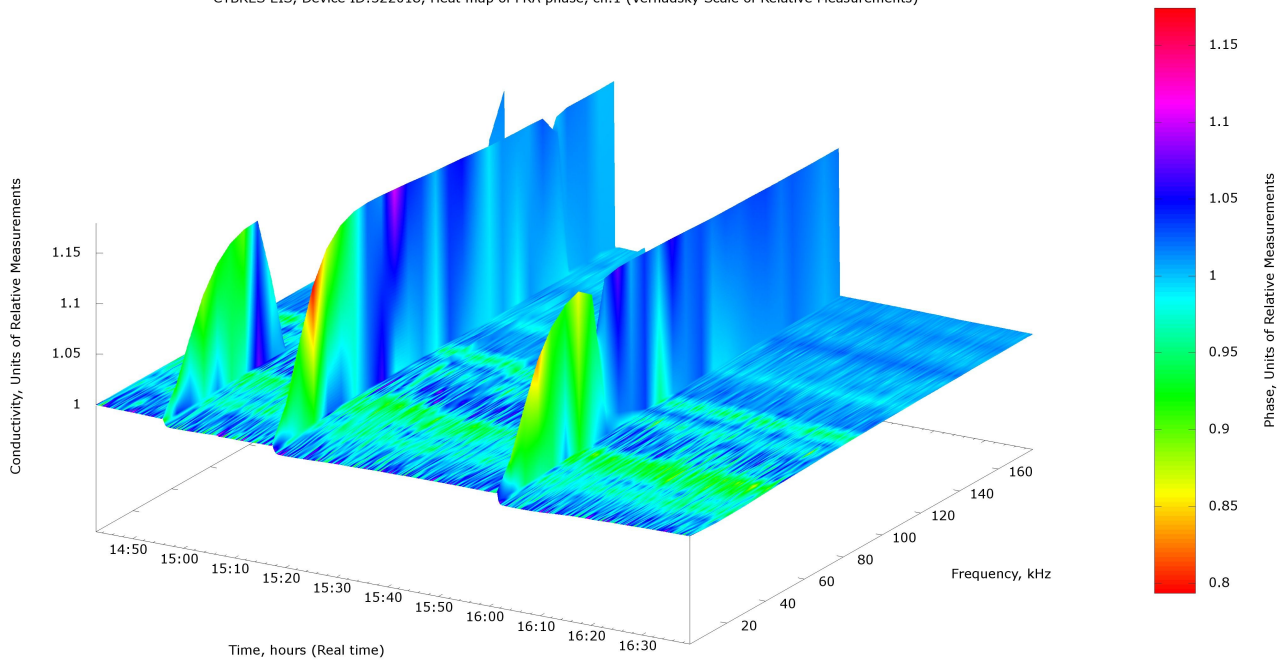


Fig. 8. The representation of RMS conductivity and FRA phase of impedance in the Vernadsky scale in the form of 4D graph, renormalization of ${}^k\varphi_t^f$ was carried out once at the beginning of measurement, the color palette HSV. The change in fluid parameters under periodic impact and their returning to the previous level are shown.

- [14] P.I. Goskov. *Metrological problems of generation and reception of torsion emission*. Reports of the 2nd International Congress, vol.2 / Ed. P.I.Goskov – Barnaul: Publishing house Alt. STU, 1999.
- [15] V.T.Shkatov. *On metrological support of torsion works (rus)*. Reports of the 5th International Congress, vol.2 / Ed. P.I.Goskov – Barnaul: Publishing house Alt. GTU, p.54-64., 2002.
- [16] M. Trukhanova and G. Shipov. The Geometro-Hydrodynamical Representation of the Torsion Field. *ArXiv e-prints*, February 2017.
- [17] M. Trukhanova. The geometro-hydrodynamical representation of the torsion field. *Physics Letters A* (doi: dx.doi.org/10.1016/j.physleta.2017.06.052), 2017.
- [18] V.P. Kaznacheev and A. Trofimov. *Reflections of Life and Intelligence on Planet Earth: Problems of Cosmo-Planetary Anthropoecology*. Academy for Future Science, 2008.